



Radiation damage conditions for ESS target hull and irradiation rigs

P. Vladimirov *, A. Möslang

*Forschungszentrum Karlsruhe, Institut für Materialforschung, Hermann-von-Helmholtz-Platz 1,
76344 Eggenstein-Leopoldshafen, Germany*

Abstract

In addition to their original mission, neutron spallation sources were also considered as a possible test bed for fusion material irradiation. Accordingly an irradiation module with 0.83 l subdivided into 10 instrumented horizontal rigs was proposed in the target–reflector interface of the ESS 5 MW long-pulse target. The irradiation conditions of this irradiation module and of the front-end target hull are given on the basis of calculations with a detailed geometry model using the neutron, photon and charged particle transport code MCNPX. Neutron and primary knock-on atom spectra, displacement damage and gas production rates as well as spallation element production rates were derived and compared with those of a fusion demonstration reactor (DEMO) and the International Fusion Materials Irradiation Facility (IFMIF). In particular, it was shown that the He/dpa ratio for the ESS reflector position is between 5 and 6 in Fe-based alloys, that is about a factor of two lower than expected for the DEMO fusion reactor. While the generation of spallation products like P, S and Ca, which are known to induce structural material embrittlement, is between 40 and 90 appm per year in the ESS target hull and is comparable with their initial concentration in the alloy, their production at the reflector position is negligibly small.

© 2005 Elsevier B.V. All rights reserved.

1. Introduction

The European spallation source – ESS was designed as an intense neutron source for various fundamental scientific applications. Besides these applications it has been suggested to evaluate whether a neutron source of this type could be potentially used as test

bed to pre-qualify candidate materials for fusion power reactors. The demand for a suitable test bed for fusion reactor materials is very large and it has stimulated the design of a dedicated high intensity neutron source – the International Fusion Materials Irradiation Facility (IFMIF), which is presently being developed under the auspices of the International Energy Agency. Nevertheless, the initial planning envisaged 4–5 years earlier availability of ESS with respect to IFMIF.

A high ranking expert group [1] evaluating the possibilities towards a ‘fast track approach to fusion energy’ came to the conclusion that besides the international facilities ITER and IFMIF it should be examined to

* Corresponding author. Tel.: +49 7247 82 4243; fax: +49 7247 82 4567.

E-mail address: pavel.vladimirov@imf.fzk.de (P. Vladimirov).

what extent relevant materials irradiation studies could be done with neutron spallation sources. Therefore, the European Fusion Development Agreement (EFDA) initiated a study to assess the pros and cons of a materials irradiation module in one of the target stations of ESS. This facility has been chosen because (a) its superior beam power promises the highest neutron fluxes and (b) it is by far easier to adopt the design of a planned project for incorporation of an irradiation module than to make the necessary changes in a facility under construction.

For investigation of fusion material behavior, an irradiation module has been proposed in the target–reflector interface region of the ESS long-pulse target as the best compromise between irradiation performance, engineering feasibility and compatibility.

In addition to this ‘reflector position’, the irradiation conditions of the front end of the target hull faced to the proton beam have been studied as well. As the target hull is the highest loaded structural material of the entire spallation source, a detailed characterization of the irradiation conditions is of primary importance for a suitable materials selection, a reliable operation of the target and an evaluation of its lifetime.

In this work we present recent results for the ESS target hull and for irradiation modules in a target–reflector position of ESS. Neutron spectra and material irradiation conditions (gas, spallation element and displacement damage production rates) will be compared with those for fusion demonstration reactor DEMO and IF-MIF [2,3].

2. Irradiation module design and set-up for transport calculations

2.1. Design of ESS irradiation module

The European spallation source is a spallation neutron source driven by a proton linear accelerator (LINAC) with beam energy of 1.33 GeV and beam power of 10 MW [4]. It features two target stations, each equipped with a liquid mercury target and operating with 5 MW beam power. The long-pulse target was suggested for housing a material test module.

For materials irradiation purposes in the long-pulse target station of ESS, a position in the lead reflector above the target (further referred as ‘reflector position’) with a useful volume of about 0.83 l has been identified [2]. The space for housing the fusion material irradiation module and its helium cooling system at ESS was limited by neutron extraction channels. As shown in Fig. 1, the module is shifted upstream as close to the channels as possible. Besides this, the position of the module was determined by the requirements

- to have sufficient neutron flux with small spatial gradients,
- to avoid high proton contribution (not relevant for fusion conditions), and
- to have an easy access to the irradiation rigs (the position above the target was selected as the most suitable).

The volume was constrained either by the necessity to house the module and its cooling ducts between neutron extraction channels or by the requirement to have suffi-

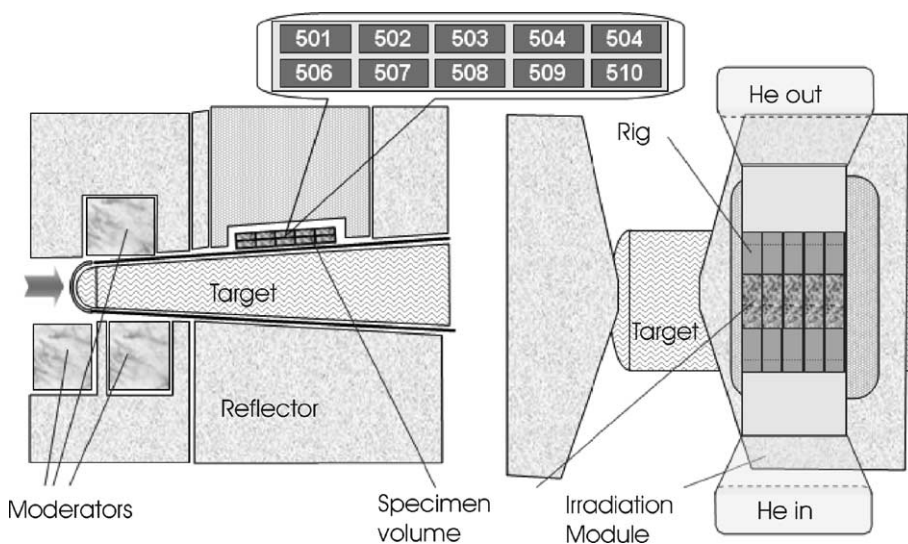


Fig. 1. Schematic view of the ESS long-pulse target: vertical (left) and horizontal (right) cuts. Irradiation rigs are incorporated in the reflector position. The numbering of rigs used for MCNPX calculation is shown in the upper insert.

cient neutron flux without large spatial gradients. Larger test volumes could be made available but at lower neutron flux level (1–3 dpa/fpy). The center of the proposed fusion materials irradiation module is positioned 38 cm downstream from the top of the liquid mercury target (Fig. 1). The irradiation module consists of 10 rectangular rigs arranged in two horizontal rows. As the suggested design concept of the ESS irradiation module is very similar to that one developed for IFMIF, the same miniaturized specimens and similar specimen capsules and coolant concepts could be used. With application of the small size specimen technology, which is being developed presently worldwide in different communities, a volume of ~ 0.83 l is sufficient for simultaneous irradiation of about 1100–1700 specimens under temperature-controlled conditions.

The rectangular rigs are helium gas cooled at the outside with low pressure (~ 0.3 MPa) but with a high gas velocity. Each rig accommodates a capsule that contains materials samples to be irradiated, similar to rigs used in fission irradiation technology (Fig. 2).

Three individual electrical heaters wrapped around each capsule are responsible for (i) a very homogeneous temperature distribution inside each capsule, and (ii) independent and adjustable individual capsule tempera-

ture [5]. Similar to many fission materials irradiation programs, the space between the test specimens inside the capsules is filled with liquid NaK for reducing temperature gradients.

Although the helium-cooled test module is designed for the irradiation of metals with specimen temperatures between 250 and 650 °C, the design allows a selection of specimen irradiation temperature in the window from less than 200 up to about 1100 °C, but at the expense of package density.

In addition to the ‘reflector position’ described above, the irradiation conditions of the front end of the target hull faced to the proton beam have been calculated.

The largest material response to irradiation is expected at the center of the beam footprint projection on the target hull surface. The irradiation conditions for this position raise considerable interest for material scientists and target designers, as it is subject to the highest irradiation loads.

2.2. Set-up for neutron and proton transport calculations

The neutron spectra for ESS have been calculated using the Monte Carlo transport code MCNPX [7], while the calculations for the IFMIF high (HFTM)

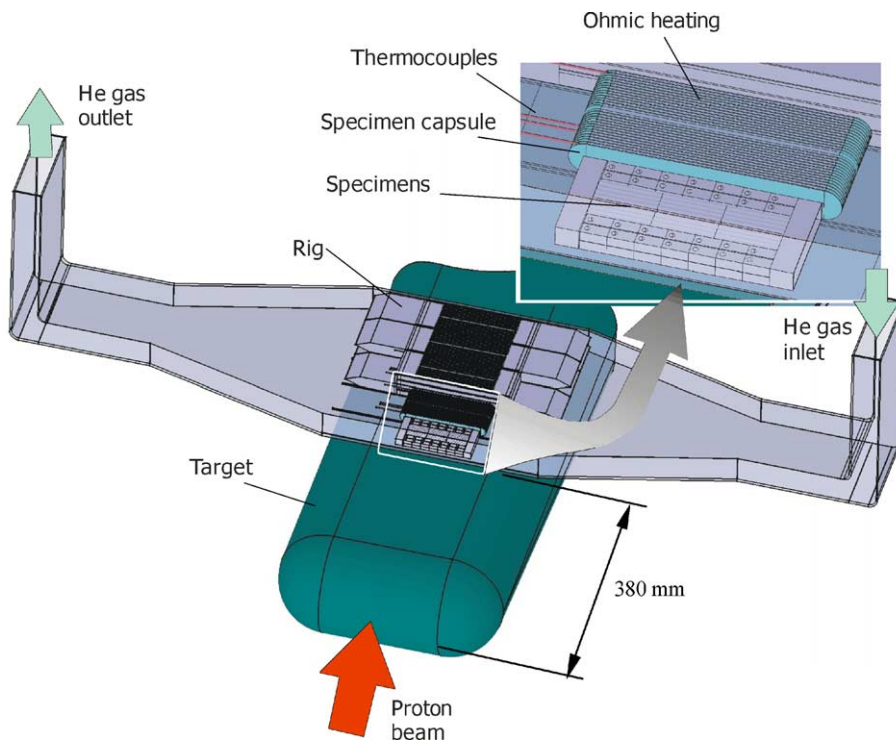


Fig. 2. Materials irradiation module with two rows of five horizontally arranged rigs on the top of the ESS long-pulse target. Each rig accommodates a temperature-controlled capsule that contains test specimens.

and medium flux test modules (MFTM) were performed by means of MCNP 4c [8] as reported previously [2,3]. The DEMO first wall spectrum was taken from Ref. [9].

The ESS target hull front was modeled as a half-cylinder perpendicular to the beam (beam footprint is elongated along the cylinder axis) ended with two quarter-spheres of the same radius.

For irradiation rigs we have estimated an average composition of 77 wt% Fe and 23 wt% He to take into account gaps between specimens and rig walls. The details on geometry model and transport calculations can be found elsewhere [2,6]. The following standard ESS beam conditions were assumed for the transport calculations: proton beam energy 1334 MeV, beam current 3.75 mA, oval beam footprint on the target $6 \times 20 \text{ cm}^2$ with Gaussian spatial distribution along both axes.

3. Results and discussion

3.1. Neutron and proton energy spectra

Fig. 3 shows a comparison of the neutron spectra at the ESS target hull front and the irradiation module at the reflector position together with the spectra for DEMO first wall and IFMIF high and medium flux test volumes.

The neutron spectrum at the front end of the target hull has a high-energy tail with energies up to the energy of incident protons (1.344 GeV). In contrast, the maximum neutron energy at the reflector position is restricted at about 500 MeV. The higher population of neutrons at the reflector position is expected and attributed to spallation neutrons, whose angular distribution is forward peaked. Therefore, one could expect more spallation neutrons at the reflector position, than at the front end

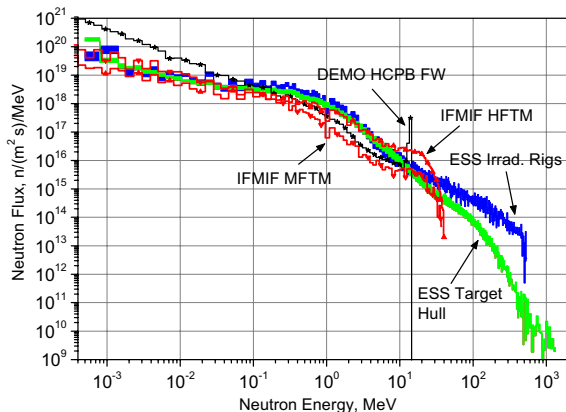


Fig. 3. Comparison of neutron differential flux densities for the ESS target hull and irradiation rigs position with those for IFMIF high and medium flux test modules and DEMO HCPB first wall.

of the target hull because only a low number of back-scattered neutrons can reach it.

The proton flux distribution was calculated inside and around the ESS target. At the center of the bottom row of irradiation rigs (cell 508) the total proton flux was calculated to be about $2.5 \times 10^{12} \text{ p/cm}^2/\text{s}$. This is only 0.4% of the total neutron flux of about $6.5 \times 10^{14} \text{ n/cm}^2/\text{s}$. However, the majority of the protons have energies far above 15 MeV and thus give a contribution to the total gas production via transmutation reactions. This helps to achieve in the irradiation rigs of the reflector position gas to dpa production ratios of about 50% of that expected under fusion neutron conditions.

Both ESS spectra have a considerable tail of neutrons with energies higher than the characteristic fusion 14 MeV peak. While the IFMIF spectrum has substantial increase around 14 MeV, both ESS spectra continuously lose their population above about 5–10 MeV without any peak in their spectra. The neutron flux at the ESS hull front is comparable with that expected for the medium flux test module (MFTM) of IFMIF, although for the ESS protons additionally affect gas, damage and spallation element production rates. The IFMIF neutron spectrum is very similar to the DEMO FW at neutron energies up to 14 MeV. In addition a neutron tail with energy up to 55 MeV is present in the IFMIF spectra which, however, is not able to produce transmutation products like P, S or Ca degrading mechanical properties of structural steels.

The results of our calculations of the material responses to irradiation are presented in Table 1. For the IFMIF MFTM the values are averaged over the entire volume, while for the helium-cooled pebble bed (HCPB) blanket of DEMO the maximum values at the first wall outboard midplane are given [9]. As the materials and design communities are most interested in structural materials irradiation performance, the irradiation conditions in individual rigs have been calculated both for the ESS irradiation module and the IFMIF high flux test module (HFTM). For the sake of easy comparison, both maximum and minimum values in different irradiation rigs are reported.

3.2. Displacement damage production rates

The results of the damage calculations are summarized in Table 1 and plotted for individual rigs in Fig. 4. The displacement damage rate in the ESS irradiation rigs is about 5–10 dpa/fpy, from which less than 0.5 dpa/fpy is produced by neutrons with energies higher than 150 MeV. Differences in damage production along each irradiation rig were calculated and appeared to be less than 5% [6]. The maximum neutron damage is observed in the cell situated in the bottom row at the position nearest to the target front. Even this maximum

Table 1
Damage, gas production rates and gas to dpa production ratio in ESS, DEMO and IFMIF

	DEMO FW (3.5 MW/m ²)	IFMIF HFTM (0.5 l)	IFMIF MFTM (6 l)	ESS target hull	ESS rigs (0.83 l)
Damage (dpa/fpy)	30	20–55	8.5	20–33	5–9.5
H production rate (appm/fpy)	1200	1000–2400	385	5×10^3 – 10^4	160–360
He production rate (appm/fpy)	330	250–600	104	500–1000	25–60
H per dpa (appm)	41	35–50	42	250–300	33–36
He per dpa (appm)	11	10–12	11	25–30	5–6

fpy stands for 'full power year'.

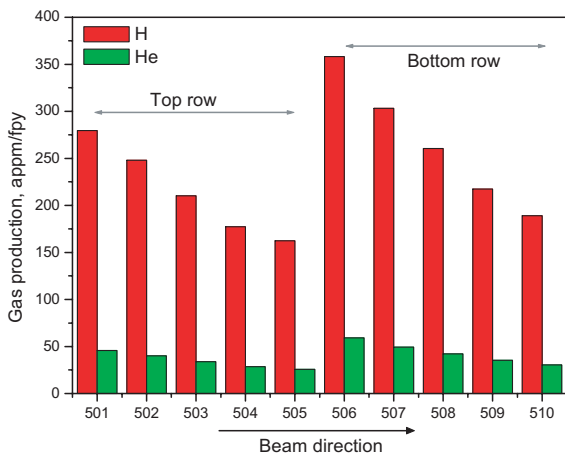


Fig. 4. Helium and hydrogen production in ESS irradiation rigs at reflector position.

value (~ 9.5 dpa/fpy) is several times lower than that for DEMO (30 dpa/fpy) and IFMIF (20–50 dpa/fpy). Therefore about three times longer irradiation campaigns will be required at ESS to reach the same DEMO relevant irradiation dose (70–80 dpa).

On the other hand, the damage rate for the target hull front is significantly higher (20–33 dpa/fpy) and reaches DEMO relevant level as expected. The contribution of the high (>150 MeV) energy nucleons to damage is about 5 dpa/fpy from 33 dpa/fpy at the target hull front and therefore much higher compared to the reflector position. It should be noted that the derived primary knock-on atom (PKA) spectra of the target hull front is a superposition of proton and neutron recoils and therefore significantly different from the only neutron induced ones of the reflector position [6]. At the target hull front the most part of spallation element and gas production as well as substantial fraction of damage originates from protons. This was supported by the results of test calculation when the spallation target was removed to simulate contribution from the source protons only. It was shown that 60–70% of gas production in the target hull is produced by the source protons. While in the case of presence of the spallation target, neutrons with energies

less than 150 MeV produce 80% of displacement damage at this position. These results for the target hull position show that source protons produce the most part of gas production, while neutrons are responsible for the major part of displacement damage.

3.3. H and He production rates

The gas production rates (H and He) in the irradiation modules of ESS are shown in Fig. 4. While the net gas production in the irradiation rigs (160–360 appm H/fpy and 25–60 appm He/fpy) is significantly lower than DEMO relevant values, the gas to dpa production ratios are only two times lower than for DEMO and IFMIF. It should be noted that these ratios could not be reached by using common material testing fission reactors in structural materials without boron or nickel addition [3]. It is remarkable that in contrast to the net gas production the gas to dpa production ratios are very slightly dependent on the position, reflecting the fact that the shape of the neutron spectrum remains unchanged, while the total neutron flux and, hence, gas production values varies from location to location within the irradiation rigs. In the IFMIF HFTM, the He/dpa and H/dpa ratios are 10–12 and 35–50, respectively and therefore practically identical to the related DEMO values.

For the ESS target hull the net gas production is higher than for DEMO and consequently the gas to dpa production ratios are also higher. The high gas production rates are mainly caused by the primary high-energy protons and are typical also for other spallation sources.

3.4. Spallation product yields

Spallation reactions induced by high-energy protons and neutrons generate a huge variety of isotopes starting from the target element down to the light elements and gaseous atoms like helium and hydrogen isotopes. Using the default MCNPX settings (Bertini–Dresner model) we have calculated spallation element production rates for pure iron at the ESS target hull and in the irradiation rigs of the reflector position. The results are presented in

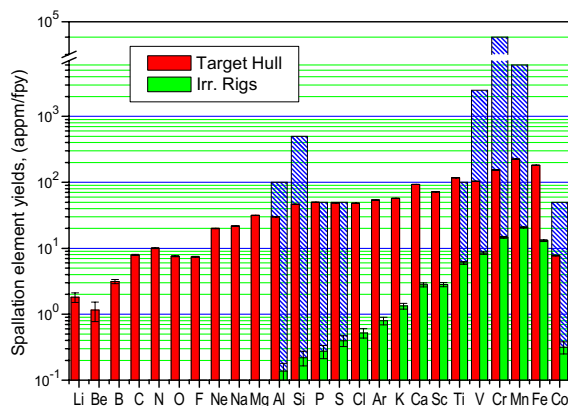


Fig. 5. Spallation element production in pure iron at the front end of the ESS target hull and at the irradiation rigs positioned in reflector. A typical f/m steel composition is shown for comparison as hatched bars (Fe amount is not shown).

Fig. 5. The harder neutron and proton spectra at the target hull produce higher spallation element production rates and include generation of elements lighter than fluorine, which are absent at the irradiation rig positions. By comparison with elemental composition of typical reduced activation ferritic–martensitic 9% Cr steels (Eurofer97) it turns out that the concentration of critical elements like phosphorous and sulfur is duplicated in the target hull after one year of irradiation. Long term experience in fission reactors has shown that both elements often accelerate irradiation embrittlement even at very low concentrations due to pronounced segregation at grain boundaries.

In contrast to the target hull, these calculations reveal only a quite moderate production of critical spallation isotopes in the reflector position. As a consequence, for reduced activation ferritic martensitic steels with limited amounts of impurity elements, the accumulation of critical spallation isotopes would not limit significantly the irradiation time at the ESS reflector position.

However, it should be noted that the spallation product yields can vary significantly with the use of different nuclear models. For comparison we have calculated spallation product yields using two semi-empirical cross-sections constructed by fitting experimental data: YIELDX [10] and EPAX [11] (see Fig. 6). The first formula (YIELDX) provides energy dependent spallation and fragmentation cross-sections for a wide range of residual and target nuclei ($3 \leq Z < 79$) and energies ($E_p > 100$ MeV). The second approach (EPAX) is energy independent and is expected to work at high energy (~ 2.2 GeV), where the energy dependence of the cross-sections is very moderate. YIELDX provides better approximation of the MCNPX results for fragments with a mass loss up to 40% (sulfur). In the intermediate mass range (phosphorous–neon) both models predict very similar results, while lower than MCNPX. The

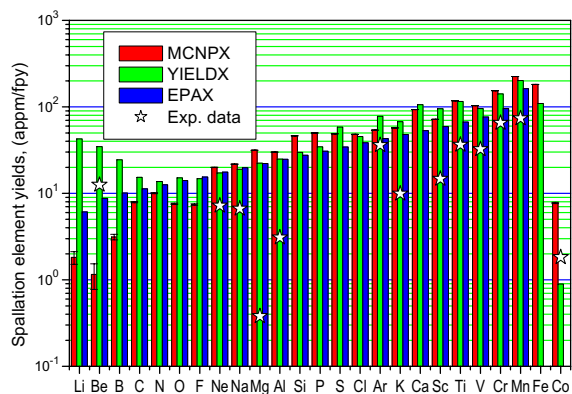


Fig. 6. Spallation element production in iron at the front end of the ESS target hull calculated by MCNPX, by semi-empirical formulae YIELDX [10] and EPAX [11] as well as using experimental cross-sections [12].

most striking difference occurs for products lighter than neon: while YIELDX predicts an increase for light element production, EPAX and MCNPX show a significant decrease. In particular, the difference in lithium and beryllium production calculated with MCNPX and YIELDX is about one order of magnitude. The experimental data from Ref. [12] are shown for comparison as well. Further comparison of different nuclear models used for spallation element production with available experimental data is necessary.

4. Summary and conclusion

In order to meet the irradiation requirements for fusion materials testing as closely as possible, a test module above the target (reflector position) with a total volume of 0.831 has been selected. The test module consists of 10 individual rigs in two horizontal rows that allow different adjustable irradiation temperatures between ~ 250 and 750 °C to be kept in each rig independently and the simultaneous irradiation of 1100–1700 qualified, miniaturized samples. Higher and lower irradiation temperatures are possible but at the expense of specimen density. In addition to this irradiation module in the reflector position, irradiation conditions at the front of the ESS target hull have been calculated and compared with those ones of a fusion DEMO reactor and IFMIF.

Based on Monte Carlo transport calculations and related nuclear data libraries, the proton induced neutron spectra revealed high-energy tails up ~ 500 MeV and ~ 1300 MeV for the reflector position and the target hull, respectively. While this high-energy tail has implications on the spallation product yields, it has almost no effect on the recoil energy distribution due to its limited population.

ESS reflector position: In spite of the high-energy tail of the spallation neutrons, the detailed MCNPX calculations showed attractive gas production conditions with 5–10 dpa/full power year and 5–6 appm He/dpa in iron-based alloys. This He/dpa ratio comes much closer to fusion blanket and IFMIF specific ratios of 10–11 appm He/dpa than any fission reactor. Also the hydrogen gas production ratio is with 33–36 appm H/dpa almost comparable with 46 appm H/dpa of a fusion DEMO first wall or with 35–50 appm He of IFMIF test modules. With respect to damage production rates, between 5 and 10 dpa/full power year can be achieved in the different rigs of the reflector position. That is, in contrast to the IFMIF high flux volume (20–55 dpa/fpy), DEMO reactor specific damage rates of ~ 30 dpa/fpa are not achievable in the ESS reflector position. Concerning spallation product yields, only a very moderate production of less than 1 appm/fpy was calculated for isotopes known to induce structural material embrittlement (like P and S), which is much below any impurity concentration of present alloys.

ESS target hull position: The displacement damage rate is with 20–33 dpa/fpy almost identical to the specific damage rate characteristic for the first wall of fusion DEMO reactor. On the other hand, mainly due to the primary high-energetic protons, the normalized hydrogen and helium production rates are 250–300 appm H/dpa and 25–30 appm He/dpa, respectively, and therefore significantly above the fusion-related ratios. Also the production rates of P and S are with 50 appm/fpy comparable to the tolerable impurity contents of typical alloys. Consequently, the irradiation loading conditions of an ESS target hull exceeds explicitly those of the Demo reactor first wall.

References

- [1] D. King (Chairman), Conclusions of the Fusion Fast Track Experts Meeting, 27 November 2001. Available from: <http://www.efda.org/downloading/debates/King_report_Dec_2001.pdf>.
- [2] A. Möslang, P. Vladimirov, Fusion material irradiation conditions in IFMIF and ESS, in: AccApp'03, Conference proceedings, San Diego, California, USA, 1–5 June 2003.
- [3] A. Möslang, P. Vladimirov, J. Nucl. Mater. 329–333 (1) (2004) 233.
- [4] G.S. Bauer, H. Ullmaier, J. Nucl. Mater. 318 (2003) 26.
- [5] S.V. Gordeev, V. Heinzl, A. Möslang and V. I. Slobodtchouk, in: AccApp 03, Conference proceedings, 1–5 June 2003, San Diego, USA.
- [6] M. Gasparotto, G. Bauer, G. Martin, A. Möslang, N. Taylor, M. Victoria, Assessment on the possibility of neutron spallation sources to contribute to the R&D program related to material irradiation testing, The Fusion Material Irradiation Devices Expert Group, EFDA-T-RE-5.0, September 2002.
- [7] L.S. Waters (Ed.), MCNPXTM Users Manual, Version 2.1.5, TPO-E83-G-UG-X-00001, Rev. 0, November 14, 1999.
- [8] J.F. Briesmeister (Ed.), MCNP – A general Monte Carlo N-particle transport code, Version 4C, LA-13709-M, Los Alamos National Laboratory, April 2000.
- [9] U. Fischer, D. Leichtle, H. Tsige-Tamirat, Neutronics characteristics of a solid breeder blanket for a fusion power demonstration reactor, in: Annual Meeting on Nuclear Technology, Karlsruhe, ISSN 0720-9207, 1999, p. 553.
- [10] R. Silberberg, C.H. Tsao, A.F. Barghouty, Astrophys. J. 501 (1998) 911.
- [11] K. Sümmerer, B. Blank, Phys. Rev. C 61 (2000) 034607.
- [12] R. Michel et al., Nucl. Instrum. and Meth. B 103 (1995) 183.